

Exploitation of Conformational Dynamics in Imparting Selective Inhibition for Related Matrix Metalloproteinases

Kiran V. Mahasenan,[†] Maria Bastian,[†] Ming Gao,[†] Emma Frost,[†] Derong Ding,[†] Katerina Zorina-Lichtenwalter,[†] John Jacobs,[†] Mark A. Suckow,[‡] Valerie A. Schroeder,[‡] William R. Wolter,[‡] Mayland Chang,^{*,†} and Shahriar Mobashery^{*,†}

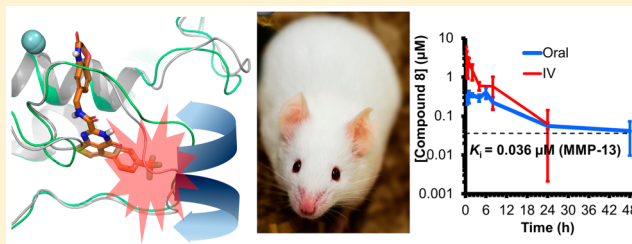
[†]Department of Chemistry and Biochemistry, University of Notre Dame, Notre Dame, Indiana 46556, United States

[‡]Freimann Life Science Center and Department of Biological Sciences, University of Notre Dame, Notre Dame, Indiana 46556, United States

S Supporting Information

ABSTRACT: Matrix metalloproteinases (MMPs) have numerous physiological functions and share a highly similar catalytic domain. Differential dynamical information on the closely related human MMP-8, -13, and -14 was integrated onto the benzoxazinone molecular template. An *in silico* library of 28,099 benzoxazinones was generated and evaluated in the context of the molecular-dynamics information. This led to experimental evaluation of 19 synthesized compounds and identification of selective inhibitors, which have potential utility in delineating the physiological functions of MMPs. Moreover, the approach serves as an example of how dynamics of closely related active sites may be exploited to achieve selective inhibition by small molecules and should find applications in other enzyme families with similar active sites.

KEYWORDS: Matrix metalloproteinases, Molecular dynamics, Virtual library design, Molecular docking, Enzyme kinetics, Animal studies



Matrix metalloproteinases (MMPs) comprise a family of 23 closely related human zinc-dependent endopeptidases with many physiological functions spanning tissue development and growth, remodeling and repair, angiogenesis, and wound healing, among others.^{1,2} The activities of these enzymes are highly regulated, and when this regulation is disrupted, MMPs manifest pathological outcomes such as cancer development and metastasis, rheumatoid arthritis, and cardiovascular and neurological diseases, to name a few.^{3,4} MMPs are evolutionarily related to each other, and their active sites share significant structural similarities.^{5,6} Indeed, these similarities explain the overlapping activities that the various members of the family exhibit, a testament to the critical functions that MMPs perform, mandating redundancy in catalysis.

Notwithstanding the documented central roles that individual MMPs play in the onset and progression of various diseases, inhibitors for MMPs have not been introduced to the market, with one exception. Doxycycline, an antibacterial agent that exhibits poor broad-spectrum MMP-inhibitory activity, is used clinically for treatment of periodontitis.^{7,8} The experience of the clinical trials of MMP inhibitors in treatment of cancer defined the essential challenge. The key impediment in the progress of these inhibitors to the clinic was the use of broad-spectrum inhibitors, which complicated treatment due to indiscriminant inhibition of many MMPs (and related zinc-dependent

enzymes), which culminated in failure in clinical trials.^{9,10} The poor outcome of these trials is reflected in the reality that in the diseased tissue one sees expressions of both the beneficial and the detrimental MMPs. A compelling example of this contrast is our recent finding that MMP-8 has a healing (beneficial) and MMP-9 a pathological (detrimental) effect in wound healing in diabetes.^{11,12} This is paradoxical. Expression of MMP-8 is the body's response to the need for wound repair, yet that of MMP-9 is a consequence of the aforementioned dysregulation. It is of interest that broad-spectrum MMP inhibition in a clinical trial of nondiabetic wounds actually showed delayed wound healing.¹³ However, highly selective MMP-9 inhibition in a rodent model of diabetic wounds sped up the healing process.^{11,12} As the details of the involvement of MMPs in these beneficial and detrimental activities will be elucidated for various MMP-mediated diseases in the future, the need for highly selective inhibitors for the MMPs as both mechanistic tools and potential therapeutics is self-evident. The present study addresses this need for highly selective MMP inhibitors.

MMPs remain as worthy targets for drug development, as long as selectivity in targeting could be imparted onto the

Received: March 23, 2017

Accepted: May 1, 2017

Published: May 1, 2017

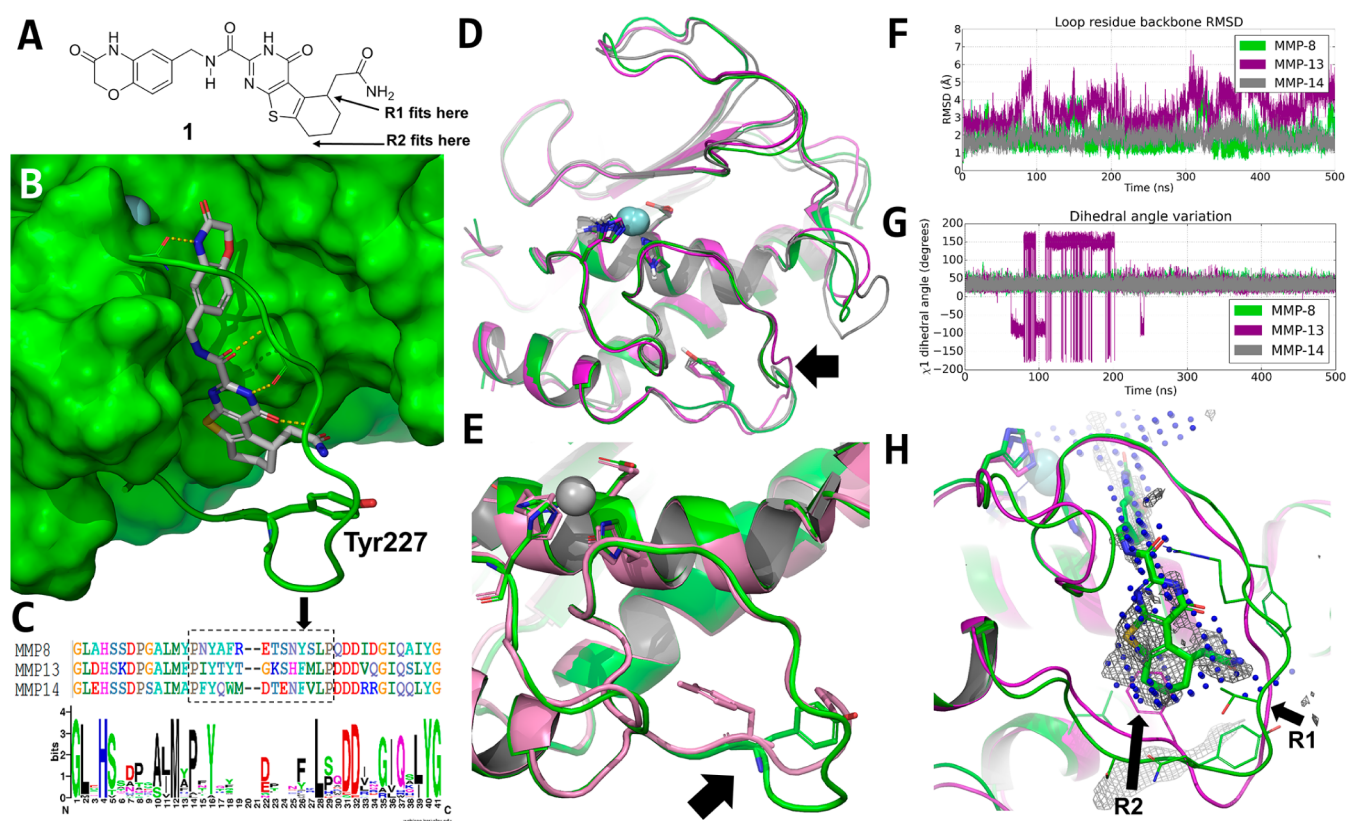


Figure 1. (A) Chemical structure of lead compound **1**. (B) X-ray structure of inhibitor **1** bound to MMP-8, showing the displaced Tyr227. Residues 218–228 of the Ω -loop are shown as a tube. (C) Sequence alignment of the catalytic domain amino acids of the 23 members of the MMP family was performed (see Figure S1), of which that for the segments of MMP-8, MMP-13, and MMP-14 are given here. The rectangular box highlights the Ω -loop residues Pro217–Pro230 for MMP-8, Pro242–Pro255 for MMP-13, and Pro259–Pro272 for MMP-14, respectively. The sequence logo (created with WebLogo v2.8¹⁶) shows the residue conservation. The arrow points to the aromatic residues within the Ω -loop critical for differentiation of the dynamics of the loop. (D) Superimposition of the X-ray crystal structures for the native Ω -loop conformations of MMP-8 (green; PDB ID: 2OY4), of MMP-13 (purple; PDB ID: 456C), and of MMP-14 (gray; PDB ID: 3MA2) shows nearly identical loop conformations (root-mean-squared deviation (RMSD) for the $C\alpha$ of loop residues of 1.6 Å for MMP-8 vs MMP-13, 0.8 Å for MMP-8 vs MMP-14, and 1.4 Å for MMP-13 vs MMP-14). The arrow points to the middle of the Ω -loops. (E) The ligand-induced MMP-8 Tyr227-out conformation (in green; PDB ID 3DNG) is superimposed to the Tyr-227-in the conformation found in the unliganded MMP-8 (PDB ID: 2OY4). The arrow points to the Tyr-227 site. (F) Time evolution of the backbone root-mean-square deviation (RMSD) of loop residues Pro242–Pro255 of MMP-13 (purple) and the corresponding residues MMP-8 (green) and MMP-14 (gray) over 500 ns molecular-dynamics simulations. (See Figure S5 of the Supporting Information for the corresponding plots for all the residues of the catalytic domain.) (G) Side-chain dihedral angle that defines rotamers based on the $C\alpha$ – $C\beta$ bond torsional axis (calculated with C – $C\alpha$ – $C\beta$ – $C\gamma$ atoms) of Tyr227 over the simulation time, along with that of corresponding residues of MMP-13 (Phe252) and of MMP-14 (Phe269). (H) Superimposition of the MMP-13 native conformation (PDB ID: 456C; purple) with that of the MMP-8-inhibitor-induced conformation (PDB ID: 3DNG; green) showing the requirement for Phe252 in MMP-13 to be displaced to accommodate the inhibitor. The structure of compound **1** is superimposed to the SiteMap binding-site-calculation result of the MMP-8 crystal structure (PDB ID: 3DNG). Blue-dot points indicate the location where ligand occupancy is favored, while the gray mesh indicates hydrophobic preference.

molecules. However, the similarities of these enzymes within their active sites have presented a formidable challenge in design of such inhibitors. Indeed, there are extraordinarily few examples of highly selective inhibitors for MMPs.^{14,15} One is the thirane class of inhibitors from our laboratory, which shows high selectivity for MMP-2 and/or MMP-9.^{17,18} Members of this class of inhibitors undergo a ring-opening reaction within the active sites of MMP-2 and MMP-9, which leads to a tight-binding inhibitor species generated within the active site.^{19,20} These inhibitors have been used widely in many animal models for MMP-2- and MMP-9-dependent diseases.^{11,21–25} Similarly, MMP-13 selective inhibitors have potential use in the study of cardiovascular diseases and osteoarthritis.^{26,27} We describe here the design of specific benzoxazinones, which target MMP-13 for selective inhibition.

The literature on inhibitors of metalloproteinases, inclusive of MMPs, is extensive.^{14,28} However, the vast majority of the inhibitor classes are zinc-ion chelators, which often suffer cross-reactivity with other enzymes. We were drawn to the previously reported benzoxazinone class of inhibitors for the reasons given below.²⁹ An X-ray structure of inhibitor **1** (Figure 1A) bound to the active site of MMP-8 (Figure 1B) showed that the compound was ensconced deep within the S1' pocket and did not directly interact with the catalytic zinc ion. The S1' pocket is present in all MMPs. It is defined by a surface, which is capped by an Ω -loop (Figure 1C). The length of the loop is variable among the MMPs (Figure S1), and from the known X-ray crystal structures, it appears to be a mobile element.^{30,31} Yet, MMP-8, MMP-13, and MMP-14 have essentially S1' loops with the identical length of 12 amino acids flanked by proline residues at each end (Figure 1C). Compound **1** inhibits MMP-

8 and MMP-13, among the eight MMPs that were evaluated.^{29,32} This observation is easily explained by the similarity of the S1' pockets in these MMPs (Table S1 and Figure S2), but that the inhibitor does not inhibit MMP-14 stood out as a noteworthy curiosity, to which we will return. In the present report, we exploit the properties of the S1' loops of the closely related MMP-8, MMP-13, and MMP-14 in arriving at molecules of the benzoxazinone class with selectivity for either MMP-8 or MMP-13. This work also sheds light on how the active site of MMP-14 is distinct, notwithstanding the seemingly high structural similarities.

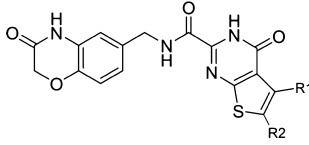
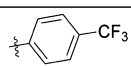
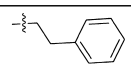
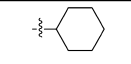
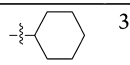
These observations argue for potential differential structural flexibility among the three active sites. In the native states of MMP-8, MMP-13, and MMP-14, with the S1' sites unoccupied, the Ω -loop adopts a comparable conformation in all three (Figure 1D). Binding of benzoxazinone **1** to the active site of MMP-8 causes a unique conformational change in the Ω -loop according to the X-ray structure (the Arg222–Ser228 stretch; Figure 1E). This observation is evidence for molecular flexibility within the active site in the case of MMP-8, but the question becomes if MMP-13 and MMP-14 also exhibit this property, or alternatively, do they have differential flexibility that could be exploited in the design of selective inhibitors. In order to assess this, we carried out molecular-dynamics simulations of MMP-8, MMP-13, and MMP-14 under identical conditions. The starting points for the simulations were the crystal structures of MMP-8, MMP-13, and MMP-14 with the Ω -loop conformations in the apoenzyme positions (Figure 1D; PDB structures 2OY4, 456C, and 3MA2, respectively). The structures were solvated with explicit water and were subjected to molecular-dynamics simulations for 500 ns using the AMBER14 suite.^{33,34} As observed by the RMSD of the Ω -loop residues over the simulation time (Figure 1F), MMP-14 showed the most stable Ω -loop. The molecular-dynamics simulation trajectory of MMP-14 revealed unique interactions of the Ω -loop residues Trp263 and Glu267 (Figure S2). The residue Trp263 of MMP-14 formed a consistent hydrogen-bonding interaction with Asn225 during the time course, while Glu267 maintained a salt-bridge with Lys146 (Figure S3). The corresponding amino acids in MMP-8 and MMP-13 are unable to make similar interactions. The MMP-13 Ω -loop showed considerable flexibility in comparison to that of MMP-8 and MMP-14. Interestingly, Phe252 of MMP-13, which corresponds to Tyr227 in MMP-8, made a dramatic motion during the simulation (see Supporting Information movie), as demonstrated by the plot of the dihedral angle corresponding to the atoms C–C α –C β –C γ that define the side-chain rotamers (Figure 1G and Figure S4). These simulations indicated that all three enzymes are different within the S1' cavity, notwithstanding the seeming similarities from the X-ray structures. The structure for MMP-14 is the most stable (static), but those of MMP-8 and MMP-13 are more flexible (dynamic). The flexibility for MMP-13 is more exaggerated compared to that for MMP-8. Such differences present challenges in inhibitor discovery, as the static crystal structure cannot guide the design. Yet, once identified, the nature of the dynamics could be exploited in opportunities for selective inhibitor design. As we describe below, this task has been accomplished in the design of selective MMP-13 inhibitors.

The use of the SiteMap program³⁵ (Schrödinger, LLC, NY, USA) on the crystal structure of the MMP-8 complex with compound **1** (PDB ID: 3DNG) indicated that the protein loci in the vicinity of the labels R1 and R2 (Figure 1A), which

underwent significant dynamics in the cases of MMP-8 and MMP-13 (Figure 1H), were promising regions for inhibitor design. The matching sites on the chemical structure of **1** were targeted for structure elaboration by molecular modeling. In preparation for this effort, a synthetically accessible virtual library of 28,099 compounds was constructed by the use of the *in silico* combinatorial library enumeration method implemented in the CombiGlide program (v. 3.2, Schrödinger, LLC, NY, USA). The analysis was based on the structural template of benzoxazinone (**1**), where the structural variations were introduced at the highlighted points (Figure 1A). Meanwhile, we computationally clustered snapshots from the 500 ns of the dynamics trajectory of MMP-13, which resulted in identification of a total of six conformations in which R1 and R2 pockets were created (See Supporting Information for method details). We docked compound **1** into these structures by the use of the Glide program³⁶ (Schrödinger, LLC, NY, USA), and the complexes were energy-minimized. We could reproduce the crystallographic fit seen for MMP-8 in two of these conformational states within 1 Å of the root-mean-squared deviation. These two conformations were then used for screening of the 28,099-strong virtual library using Glide. The compounds were ranked for the goodness of fit, but were eliminated, if they did not conform to Lipinski's rule of five³⁷ and Jorgensen's rule of three.^{38–40} With synthetic access (and availability of the starting materials) being a final filter, we selected for synthesis 19 of the high-ranking compounds (See Supporting Information for method details).

Five of the target compounds are given in Table 1; an additional 14 compounds are shown in the Supporting Information (Figure S6). We highlight the five-step synthesis

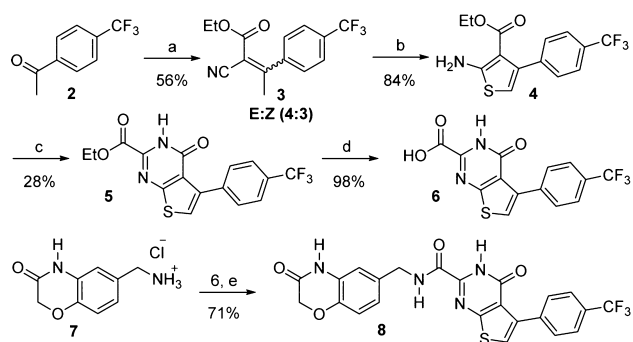
Table 1. Kinetic Parameters for Inhibition of MMPs

	R1	R2	K_i (nM)		
			MMP-8	MMP-13	MMP-14
1 ^{*32}					
8		H	8500 ± 1400	36 ± 11	1% ^a
9		H	6500 ± 900	190 ± 14	4% ^a
10		H	19 ± 5	0.47 ± 0.06	14% ^a
11	H		3.3 ± 0.2	24.5 ± 3	57% ^b
12			0.71 ± 0.04	0.59 ± 0.07	14% ^a

^aInhibition at 10 μ M. ^bInhibition at 50 μ M. ^{*}Racemic mixture (R, S).

of compound **8** below (Scheme 1). The synthesis is a variation of a reported method for compound **1**.³² 1-(4-

Scheme 1. Synthesis of Inhibitor **8**^a



^aReagents and conditions: (a) $\text{NCCH}_2\text{COOEt}$, toluene, 140 °C. (b) S, HNEt_2 , MeOH, 50 °C. (c) NCCO_2Et , HCl, dioxane, 50 °C. (d) LiOH, THF, rt. (e) HATU, NMM, DMF, rt.

(Trifluoromethyl)phenylethan-1-one (**2**) and ethyl cyanoacetate were heated in toluene to afford the α,β -unsaturated ethyl ester **3** as a mixture of *E*- and *Z*-isomers. This isomeric mixture was allowed to react with elemental sulfur to give **4**. The reaction of ethyl cyanoformate in the presence of acid afforded compound **5**. Subsequent hydrolysis of the ethyl ester of **5** resulted in compound **6**. Coupling of **6** and amine **7**, which itself was synthesized in three steps according to the literature,³² afforded the desired product **8**.

The synthetic compounds were evaluated for their *in vitro* enzyme inhibition on a panel of eight representative MMPs. A rapid up-front screening was conducted by incubating the compounds at 10 μM with the corresponding enzymes and the requisite substrates. Those compounds that showed >50% inhibition were further evaluated, and their dissociation constants (K_i) were determined (Table 1 and Table S2). These compounds showed marginal to no inhibition of MMP-1, MMP-2, MMP-3, MMP-7, MMP-9, and MMP-14.

Compound **8** emerged as the most selective for MMP-13 among the synthesized compounds. This compound is a competitive inhibitor with 240-fold selectivity for MMP-13 over MMP-8 (K_i of 36 ± 11 nM vs 8500 ± 1400 nM). Similarly, compounds **9** and **10** showed 35- and 40-fold selectivity, respectively, for MMP-13 over MMP-8 (compound **9**, 190 ± 14 nM vs 6500 ± 900 nM; compound **10**, 0.47 ± 0.06 nM vs 19 ± 5 nM). The activities of these two compounds indicated the importance of hydrophobic bulky substitution in this region for MMP-13 selectivity. Selectivity in inhibition by compound **11** was switched in favor of MMP-8, as opposed to MMP-13, but only modestly so. On the other hand, compound **12** inhibited MMP-8 and MMP-13 equally well and equally potently (subnanomolar inhibition).

The thienopyrimidinone cyclic system, connected to the benzoxazinone scaffold via the amide linker was substituted with other diverse groups in the rest of the compounds reported here (**13**–**26**, Supporting Information Figure S6 and Table S2). Pyrazole substitution (compound **13**, **14**, **15**) resulted in loss in binding affinity from nanomolar to micromolar level, but demonstrated weak selectivity for MMP-13. Compound **13**, with bulkier naphthalene ring occupying the S1' site, showed 4-fold preference for MMP-13 over compounds **14** and **15**, with smaller substitutions (phenyl

and thiophene, respectively). These compounds showed weaker inhibition for MMP-8, likely due to their less flexible and thus unaccommodating S1' site. These findings collectively suggest the requirement of a bulkier rigid hydrophobic group that can replace the Tyr/Phe for the S1' site and accommodate the pocket for inhibition. We note that not all the synthesized compounds showed inhibitory properties for the panel of the enzymes that was screened, which is the limitation of the method, but the properties of compound **8** fit the traits that we set out to identify: selectivity for MMP-13 over MMP-8 and lack of inhibition of MMP-14. Although our repeated efforts in crystallography of compound **8** with MMP-13 did not succeed, the potent *in vitro* inhibition data support direct binding of the compound to the target.

The pharmacokinetic properties of compound **8** were assessed in mice ($n = 3$ mice per time point per route of administration, total 54 mice) after intravenous (iv) and oral (po) dose administration (Figure 2, and Supporting Informa-

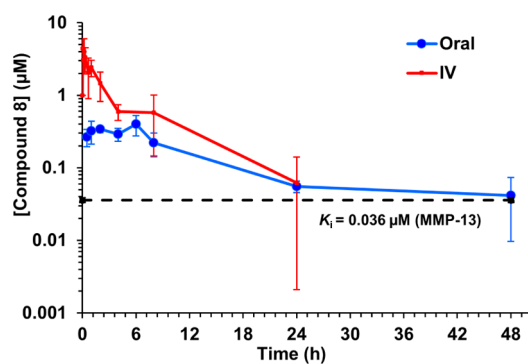


Figure 2. Plasma concentration–time curves after a single 1 mg/kg intravenous (iv, red) dose and 10 mg/kg oral (po, blue) dose administration of compound **8** in mice ($n = 3$ per time point per route of administration, total 54 mice).

tion). After a single 1 mg/kg iv dose of **8**, the plasma concentration was 4.4 ± 1.6 μM at 2 min and remained above the K_i for MMP-13 at 24 h (0.062 ± 0.078 μM). Compound **8** had $\text{AUC}_{0-\infty}$ of 889 $\mu\text{M}\cdot\text{min}$, low clearance (CL) of 2.2 mL/min/kg (3% of hepatic blood flow), high volume of distribution (V_d) of 1.0 L/kg, and an elimination half-life of 5.3 h. After a 10 mg/kg po dose, the maximum plasma concentration was 0.40 ± 0.13 μM at 6 h and declined to 0.042 ± 0.032 μM at 48 h; however, it was above K_i for MMP-13. The elimination half-life was 17.5 h. $\text{AUC}_{0-\infty}$ was 415 $\mu\text{M}\cdot\text{min}$. Comparison of the AUC after po to that after iv gave an absolute oral bioavailability of 4.7%, after dose adjustment.

In conclusion, we report here an example of how crystallographically similar binding sites may be exploited for selective inhibitor design based on their dynamic nature. Our computational simulations offered insights on the flexibility of the structurally similar binding sites of MMP-8, MMP-13, and MMP-14. Encouraged by the opportunity offered by this simulation, a virtual focused library was designed and evaluated *in silico*. Synthesis and *in vitro* evaluation of a subset of the library successfully identified compounds with desired activity. The kinetic data clearly document that selectivity based on the design paradigm is achievable. The compound disclosed herein has favorable *in vivo* pharmacokinetic properties in mice and can potentially serve as a useful tool for delineating the functions of the MMP family of enzymes.

■ ASSOCIATED CONTENT

● Supporting Information

The Supporting Information is available free of charge on the ACS Publications website at DOI: 10.1021/acsmedchemlett.7b00130.

The Ω -loop sequence alignment of 23 members of the human MMP family, binding-site comparison of MMP-8, MMP-13, and MMP-14, structures and activities of compounds, methods for MD simulations, *in silico* library design, virtual screening, syntheses and characterization of compounds, enzyme inhibition studies, and pharmacokinetic studies (PDF)

Movie of MD simulation (AVI)

■ AUTHOR INFORMATION

Corresponding Authors

*M.C.: E-mail, mchang@nd.edu; Phone, +1-574-631-2965.

*S.M.: E-mail, mobashery@nd.edu; Phone, +1-574-631-2933.

ORCID

Shahriar Mobashery: 0000-0002-7695-7883

Funding

This work was supported in part by the Craig H. Nielsen Foundation (grant 282987 to M.C.).

Notes

The authors declare no competing financial interest.

■ ACKNOWLEDGMENTS

We acknowledge computing resources and assistance provided by Center for Research Computing of the University of Notre Dame.

■ ABBREVIATIONS

HATU, 1-[bis(dimethylamino)methylene]-1H-1,2,3-triazolo[4,5-*b*]pyridinium 3-oxide hexafluorophosphate; iv, intravenous; MD, molecular dynamics; MMP, matrix metalloproteinase; NMM, 4-methylmorpholine; po, per os; RMSD, root-mean-squared deviation; UPLC, ultraperformance liquid chromatography; UV, ultraviolet

■ REFERENCES

- (1) Klein, T.; Bischoff, R. Physiology and pathophysiology of matrix metalloproteases. *Amino Acids* **2011**, *41*, 271–290.
- (2) Pulkoski-Gross, A. E. Historical perspective of matrix metalloproteases. *Front. Biosci., Scholar Ed.* **2015**, *7*, 125–149.
- (3) Tauro, M.; McGuire, J.; Lynch, C. C. New approaches to selectively target cancer-associated matrix metalloproteinase activity. *Cancer Metastasis Rev.* **2014**, *33*, 1043–1057.
- (4) Vandenbroucke, R. E.; Libert, C. Is there new hope for therapeutic matrix metalloproteinase inhibition? *Nat. Rev. Drug Discovery* **2014**, *13*, 904–927.
- (5) Fanjul-Fernandez, M.; Folgueras, A. R.; Cabrera, S.; Lopez-Otin, C. Matrix metalloproteinases: evolution, gene regulation and functional analysis in mouse models. *Biochim. Biophys. Acta, Mol. Cell Res.* **2010**, *1803*, 3–19.
- (6) Massova, I.; Kotra, L. P.; Fridman, R.; Mobashery, S. Matrix metalloproteinases: structures, evolution, and diversification. *FASEB J.* **1998**, *12*, 1075–1095.
- (7) Peterson, J. T. Matrix metalloproteinase inhibitor development and the remodeling of drug discovery. *Heart Failure Rev.* **2004**, *9*, 63–79.
- (8) Sorsa, T.; Tjaderhane, L.; Konttinen, Y. T.; Lauhio, A.; Salo, T.; Lee, H. M.; Golub, L. M.; Brown, D. L.; Mantyla, P. Matrix

metalloproteinases: contribution to pathogenesis, diagnosis and treatment of periodontal inflammation. *Ann. Med.* **2006**, *38*, 306–321.

- (9) Cathcart, J. M.; Cao, J. MMP Inhibitors: Past, present and future. *Front. Biosci., Landmark Ed.* **2015**, *20*, 1164–1178.

- (10) Dufour, A.; Overall, C. M. Missing the target: matrix metalloproteinase antitargets in inflammation and cancer. *Trends Pharmacol. Sci.* **2013**, *34*, 233–242.

- (11) Gao, M.; Nguyen, T. T.; Suckow, M. A.; Wolter, W. R.; Gooyit, M.; Mobashery, S.; Chang, M. Acceleration of diabetic wound healing using a novel protease-anti-protease combination therapy. *Proc. Natl. Acad. Sci. U. S. A.* **2015**, *112*, 15226–15231.

- (12) Gooyit, M.; Peng, Z.; Wolter, W. R.; Pi, H.; Ding, D.; Heseck, D.; Lee, M.; Boggess, B.; Champion, M. M.; Suckow, M. A.; Mobashery, S.; Chang, M. A chemical biological strategy to facilitate diabetic wound healing. *ACS Chem. Biol.* **2014**, *9*, 105–110.

- (13) Agren, M. S.; Mirastschijski, U.; Karlsmark, T.; Saarialho-Kere, U. K. Topical synthetic inhibitor of matrix metalloproteinases delays epidermal regeneration of human wounds. *Exp. Dermatol.* **2001**, *10*, 337–348.

- (14) Fisher, J. F.; Mobashery, S. Recent advances in MMP inhibitor design. *Cancer Metastasis Rev.* **2006**, *25*, 115–136.

- (15) Jacobsen, J. A.; Major Jourden, J. L.; Miller, M. T.; Cohen, S. M. To bind zinc or not to bind zinc: an examination of innovative approaches to improved metalloproteinase inhibition. *Biochim. Biophys. Acta, Mol. Cell Res.* **2010**, *1803*, 72–94.

- (16) Crooks, G. E.; Hon, G.; Chandonia, J. M.; Brenner, S. E. WebLogo: a sequence logo generator. *Genome Res.* **2004**, *14*, 1188–1190.

- (17) Gooyit, M.; Song, W.; Mahasenan, K. V.; Lichtenwalter, K.; Suckow, M. A.; Schroeder, V. A.; Wolter, W. R.; Mobashery, S.; Chang, M. O-phenyl carbamate and phenyl urea thiiranes as selective matrix metalloproteinase-2 inhibitors that cross the blood-brain barrier. *J. Med. Chem.* **2013**, *56*, 8139–8150.

- (18) Gooyit, M.; Peng, Z.; Mobashery, S.; Chang, M. *Thiirane Class of Gelatinase Inhibitors as a Privileged Template that Crosses the Blood-Brain Barrier*; Royal Society of Chemistry Publishing, 2016; pp 262–286.

- (19) Forbes, C.; Shi, Q.; Fisher, J. F.; Lee, M.; Heseck, D.; Llarrull, L. I.; Toth, M.; Gossing, M.; Fridman, R.; Mobashery, S. Active site ring-opening of a thiirane moiety and picomolar inhibition of gelatinases. *Chem. Biol. Drug Des.* **2009**, *74*, 527–534.

- (20) Tao, P.; Fisher, J. F.; Shi, Q.; Vreven, T.; Mobashery, S.; Schlegel, H. B. Matrix metalloproteinase 2 inhibition: combined quantum mechanics and molecular mechanics studies of the inhibition mechanism of (4-phenoxyphenylsulfonyl)methylthiirane and its oxirane analogue. *Biochemistry* **2009**, *48*, 9839–9847.

- (21) Cui, J.; Chen, S.; Zhang, C.; Meng, F.; Wu, W.; Hu, R.; Hadass, O.; Lehmid, T.; Blair, G. J.; Lee, M.; Chang, M.; Mobashery, S.; Sun, G. Y.; Gu, Z. Inhibition of MMP-9 by a selective gelatinase inhibitor protects neurovasculature from embolic focal cerebral ischemia. *Mol. Neurodegener.* **2012**, *7*, 21.

- (22) Gu, Z.; Cui, J.; Brown, S.; Fridman, R.; Mobashery, S.; Strongin, A. Y.; Lipton, S. A. A highly specific inhibitor of matrix metalloproteinase-9 rescues laminin from proteolysis and neurons from apoptosis in transient focal cerebral ischemia. *J. Neurosci.* **2005**, *25*, 6401–6408.

- (23) Hadass, O.; Tomlinson, B. N.; Gooyit, M.; Chen, S.; Purdy, J. J.; Walker, J. M.; Zhang, C.; Giritharan, A. B.; Purnell, W.; Robinson, C. R., 2nd; Shin, D.; Schroeder, V. A.; Suckow, M. A.; Simonyi, A.; Sun, G. Y.; Mobashery, S.; Cui, J.; Chang, M.; Gu, Z. Selective inhibition of matrix metalloproteinase-9 attenuates secondary damage resulting from severe traumatic brain injury. *PLoS One* **2013**, *8*, e76904.

- (24) Lee, M.; Chen, Z.; Tomlinson, B. N.; Gooyit, M.; Heseck, D.; Juarez, M. R.; Nizam, R.; Boggess, B.; Lastochkin, E.; Schroeder, V. A.; Wolter, W. R.; Suckow, M. A.; Cui, J.; Mobashery, S.; Gu, Z.; Chang, M. Water-Soluble MMP-9 Inhibitor Reduces Lesion Volume after Severe Traumatic Brain Injury. *ACS Chem. Neurosci.* **2015**, *6*, 1658–1664.

(25) Marusak, C.; Bayles, I.; Ma, J.; Gooyit, M.; Gao, M.; Chang, M.; Bedogni, B. The thiirane-based selective MT1-MMP/MMP2 inhibitor ND-322 reduces melanoma tumor growth and delays metastatic dissemination. *Pharmacol. Res.* **2016**, *113*, 515–520.

(26) Austin, K. M.; Covic, L.; Kuliopulos, A. Matrix metalloproteases and PAR1 activation. *Blood* **2013**, *121*, 431–439.

(27) Li, N. G.; Shi, Z. H.; Tang, Y. P.; Wang, Z. J.; Song, S. L.; Qian, L. H.; Qian, D. W.; Duan, J. A. New hope for the treatment of osteoarthritis through selective inhibition of MMP-13. *Curr. Med. Chem.* **2011**, *18*, 977–1001.

(28) Georgiadis, D.; Yiotakis, A. Specific targeting of metzincin family members with small-molecule inhibitors: progress toward a multifarious challenge. *Bioorg. Med. Chem.* **2008**, *16*, 8781–8794.

(29) Pochetti, G.; Montanari, R.; Gege, C.; Chevrier, C.; Taveras, A. G.; Mazza, F. Extra binding region induced by non-zinc chelating inhibitors into the S1' subsite of matrix metalloproteinase 8 (MMP-8). *J. Med. Chem.* **2009**, *52*, 1040–1049.

(30) Fabre, B.; Ramos, A.; de Pascual-Teresa, B. Targeting matrix metalloproteinases: exploring the dynamics of the s1' pocket in the design of selective, small molecule inhibitors. *J. Med. Chem.* **2014**, *57*, 10205–10219.

(31) Devel, L.; Czarny, B.; Beau, F.; Georgiadis, D.; Stura, E.; Dive, V. Third generation of matrix metalloprotease inhibitors: Gain in selectivity by targeting the depth of the S1' cavity. *Biochimie* **2010**, *92*, 1501–1508.

(32) Ding, D. R.; Lichtenwalter, K.; Pi, H. L.; Mobashery, S.; Chang, M. Characterization of a selective inhibitor for matrix metalloproteinase-8 (MMP-8). *MedChemComm* **2014**, *5*, 1381–1383.

(33) Gotz, A. W.; Williamson, M. J.; Xu, D.; Poole, D.; Le Grand, S.; Walker, R. C. Routine Microsecond Molecular Dynamics Simulations with AMBER on GPUs. 1. Generalized Born. *J. Chem. Theory Comput.* **2012**, *8*, 1542–1555.

(34) Case, D. A.; Babin, V.; Berryman, J. T.; Betz, R. M.; Cai, Q.; Cerutti, D. S.; Cheatham, T. E.; Darden, T. A.; Duke, R. E.; Gohlke, H.; Goetz, A. W.; Gusarov, S.; Homeyer, N.; Janowski, P.; Kaus, J.; Kolossváry, I.; Kovalenko, A.; Lee, T. S.; LeGrand, S.; Luchko, T.; Luo, R.; Madej, B.; Merz, K. M.; Paesani, F.; Roe, D. R.; Roitberg, A.; Sagui, C.; Salomon-Ferrer, R.; Seabra, G.; Simmerling, C. L.; Smith, W.; Swails, J.; Walker, J.; Wang, J.; Wolf, R. M.; Wu, X.; Kollman, P. A. *AMBER 2014*; University of California, San Francisco, 2014.

(35) Halgren, T. A. Identifying and characterizing binding sites and assessing druggability. *J. Chem. Inf. Model.* **2009**, *49*, 377–389.

(36) Friesner, R. A.; Banks, J. L.; Murphy, R. B.; Halgren, T. A.; Klicic, J. J.; Mainz, D. T.; Repasky, M. P.; Knoll, E. H.; Shelley, M.; Perry, J. K.; Shaw, D. E.; Francis, P.; Shenkin, P. S. Glide: a new approach for rapid, accurate docking and scoring. 1. Method and assessment of docking accuracy. *J. Med. Chem.* **2004**, *47*, 1739–1749.

(37) Lipinski, C. A.; Lombardo, F.; Dominy, B. W.; Feeney, P. J. Experimental and computational approaches to estimate solubility and permeability in drug discovery and development settings. *Adv. Drug Delivery Rev.* **2001**, *46*, 3–26.

(38) Jorgensen, W. L.; Duffy, E. M. Prediction of drug solubility from structure. *Adv. Drug Delivery Rev.* **2002**, *54*, 355–366.

(39) Roe, D. R.; Cheatham, T. E., 3rd. PTRAJ and CPPTRAJ: Software for Processing and Analysis of Molecular Dynamics Trajectory Data. *J. Chem. Theory Comput.* **2013**, *9*, 3084–3095.

(40) Page-McCaw, A.; Ewald, A. J.; Werb, Z. Matrix metalloproteinases and the regulation of tissue remodelling. *Nat. Rev. Mol. Cell Biol.* **2007**, *8*, 221–233.